Journal of The Electrochemical Society, **151** (11) A1899-A1904 (2004)

0013-4651/2004/151(11)/A1899/6/$7.00 © The Electrochemical Society, Inc.

A1899

Synthesis, Thermal, and Electrochemical Properties of AlPO$_4$-Coated LiNi$_{0.8}$Co$_{0.1}$Mn$_{0.1}$O$_2$ Cathode Materials for a Li-Ion Cell

Jaephil Cho,[a,*,z] Tae-Joon Kim,[b] Jisuk Kim,[a] Mijung Noh,[a] and Byungwoo Park[b]

[a]*Department of Applied Chemistry, Kumoh National Institute of Technology, Gumi 730-701, Korea*
[b]*School of Materials Science and Engineering and Research Center for Energy Conversion and Storage, Seoul National University, Seoul, Korea*

Although LiNi$_{0.8}$Co$_{0.1}$Mn$_{0.1}$O$_2$ cathode material has a larger specific capacity than LiCoO$_2$, their thermal instability has hindered their use in Li-ion cells. An AlPO$_4$ coating on the LiNi$_{0.8}$Co$_{0.1}$Mn$_{0.1}$O$_2$ cathode, however, noticeably diminished the violent exothermic reaction of the cathode material with the electrolyte, without sacrificing the specific capacity of the bare LiNi$_{0.8}$Co$_{0.1}$Mn$_{0.1}$O$_2$ (188 mAh/g at 4.3 V charge cut off). The results were consistent with the thermal abuse tests using Li-ion cells; the AlPO$_4$-coated LiNi$_{0.8}$Co$_{0.1}$Mn$_{0.1}$O$_2$ cathode did not exhibit thermal runaway with smoke and explosion, in contrast to the cell containing the bare cathode. In addition, the AlPO$_4$-coated LiNi$_{0.8}$Co$_{0.1}$Mn$_{0.1}$O$_2$ cathode exhibited a superior cycle-life performance compared to the bare LiNi$_{0.8}$Co$_{0.1}$Mn$_{0.1}$O$_2$.
© 2004 The Electrochemical Society. [DOI: 10.1149/1.1802411] All rights reserved.

Manuscript submitted October 28, 2003; revised manuscript received April 12, 2004. Available electronically October 21, 2004.

Many studies of Ni-based cathode materials (LiNi$_{1-x}$M$_x$O$_2$ where M = metals) have generally been focused on improving the electrochemical properties of the material by a partial substitution of Ni with another transition metal (rather than improving the thermal stability).[1-7] For example, the substitution of Ni with Co up to x = 0.5 has been reported to improve its structural stability on cycling, although the substitution slightly reduces the electrochemical capacity. Such an improvement is understood to be due to the reduction of hexagonal and monoclinic phase transitions that cause NiO$_2$ layer distortion at voltages above 4 V.[8-12] In terms of the thermal stability of the LiNi$_{1-x}$M$_x$O$_2$ cathodes, a violent exothermic reaction of the cathode with the electrolyte accompanied by substantial heat generation should be avoided. Otherwise, it causes thermal runaway exhibiting fire, sparks and an explosion. In order to minimize the amount of oxygen evolution (heat generation) via the exothermic reaction, the addition of Mg, Ti, or Al in LiNiO$_2$ was reported to be effective, but it greatly sacrifices the discharge capacity.[13,14] Another problem in Ni-based cathode materials is that its average cell voltage is lower than LiCoO$_2$ by approximately 0.1-0.2 V. Hence, the specific capacity of Ni-based cathodes should be ~5% higher than LiCoO$_2$, to compensate for the low working voltage.
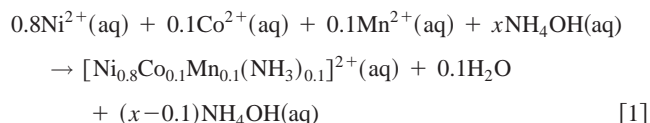
As yet, Ni-based cathode materials have not met the safety guidelines requiring no explosion, fire, and smoke during the nail penetration test at the 4.35 V charged state in the Li-ion cell.[15] In order to overcome this technical hurdle, some additives (for example, γ-butyrolacetone) were used to reduce the direct reaction of the cathode with the electrolyte at the charged state. This solvent was reported to decompose into the organic products, which encapsulate the cathode, thereby blocking any direct reaction with the electrolyte.[16] As a consequence, Li-ion cells containing this solvent did not explode during the nail penetration tests at 4.35 V and the overcharging tests to 12 V. However, the additives decreased the cycle life performance and rate capability. Therefore, its electrochemical properties still need to be customized. Recently, a more fundamental approach for improving the thermal instability of the cathode materials has been reported by Cho *et al.*[17] They demonstrated that a nanoparticle-AlPO$_4$ coating on the LiCoO$_2$ cathodes blocked the thermal runaway of the Li-ion cell, and significantly reduced the electrolyte oxidation and Co dissolution into the electrolyte. However, this study showed the enhanced 12 V overcharge behavior of the LiCoO$_2$ cathode by AlPO$_4$ coating, without other

important thermal abuse tests such as nail penetration, systematic overcharge, and differential scanning calorimetry (DSC) results.
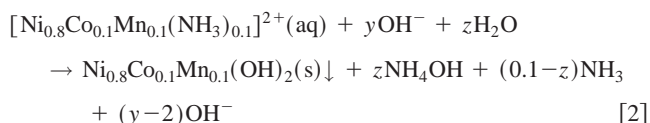
In this paper, we report the synthesis and thermal/electrochemical properties of AlPO$_4$-coated LiNi$_{0.8}$Co$_{0.1}$Mn$_{0.1}$O$_2$ cathodes for the first time. Appropriate stoichiometry of LiNi$_{1-x-y}$Co$_x$Mn$_y$O$_2$ was selected in this work with a small amount of Co and Mn, not to sacrifice the discharge capacity, and to guarantee the structural stability during deep charging. In particular, this study demonstrates that a nanoparticle coating on the cathode suppresses the upsurge of oxygen generation from the LiNi$_{0.8}$Co$_{0.1}$Mn$_{0.1}$O$_2$ cathode. In addition, a direct comparison of nail penetration and 12 V overcharge results were not tried before, although these are very critical evaluation techniques for the cathodes in Li-ion cells. The starting material Ni$_{0.8}$Co$_{0.1}$Mn$_{0.1}$(OH)$_2$ for preparing the cathode was coprecipitated from solution, which has a great advantage over the conventional sol-gel method for controlling the particle size and Brunauer-Emmett-Teller (BET) surface area.

Experimental

Synthesis of Ni$_{0.8}$Co$_{0.1}$Mn$_{0.1}$(OH)$_2$ and LiNi$_{0.8}$Co$_{0.1}$Mn$_{0.1}$O$_2$.—Ni$_{0.8}$Co$_{0.1}$Mn$_{0.1}$(OH)$_2$ starting powders consisting of spherical particles (~13 μm in diameter) were prepared by coprecipitation from a solution containing stoichiometric amounts of nickel/cobalt/manganese nitrates by the addition of NaOH and NH$_4$OH solution in a specially designed reactor for spherical particles according to the reactions[18]

$$0.8\text{Ni}^{2+}(\text{aq}) + 0.1\text{Co}^{2+}(\text{aq}) + 0.1\text{Mn}^{2+}(\text{aq}) + x\text{NH}_4\text{OH}(\text{aq})$$
$$\rightarrow [\text{Ni}_{0.8}\text{Co}_{0.1}\text{Mn}_{0.1}(\text{NH}_3)_{0.1}]^{2+}(\text{aq}) + 0.1\text{H}_2\text{O}$$
$$+ (x-0.1)\text{NH}_4\text{OH}(\text{aq}) \qquad [1]$$

and

$$[\text{Ni}_{0.8}\text{Co}_{0.1}\text{Mn}_{0.1}(\text{NH}_3)_{0.1}]^{2+}(\text{aq}) + y\text{OH}^- + z\text{H}_2\text{O}$$
$$\rightarrow \text{Ni}_{0.8}\text{Co}_{0.1}\text{Mn}_{0.1}(\text{OH})_2(\text{s})\downarrow + z\text{NH}_4\text{OH} + (0.1-z)\text{NH}_3$$
$$+ (y-2)\text{OH}^- \qquad [2]$$

The Ni$_{0.8}$Co$_{0.1}$Mn$_{0.1}$(OH)$_2$ particle size was controlled by the reaction time in order to enhance the BET surface area. A longer reaction time in the solution resulted in a larger particle size. The coprecipitated particles continued to be rotated at 1000 rpm in the reactor at 50°C. The pH was maintained at 11.5 by controlling the amount of NaOH. Coprecipitation methods are industrially well known. Ohzuku *et al.* used commercial hydroxide precursors.[19] On the other

* Electrochemical Society Active Member.
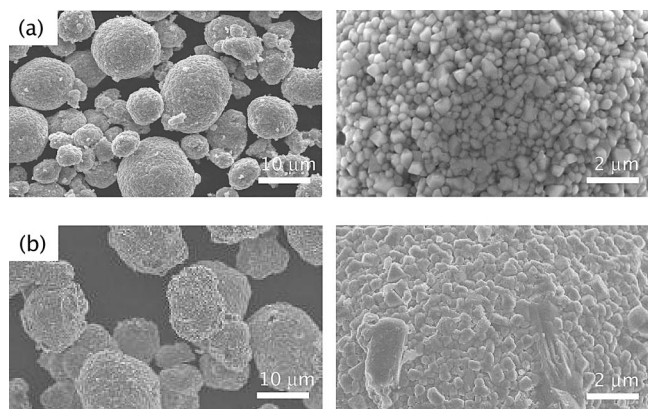z E-mail: jpcho@kumoh.ac.kr

Figure 1. SEM micrographs of (a) bare and (b) $AlPO_4$-coated $LiNi_{0.8}Co_{0.1}Mn_{0.1}O_2$ powders.

hand, Dahn's group used the coprecipitation method by controlling with $LiOH$,[20] and their recipe could not yield high density. However, we obtained spherical powders with high density through the coprecipitation method by controlling with NH_4OH and $NaOH$.

$LiNi_{0.8}Co_{0.1}Mn_{0.1}O_2$ was prepared by mixing stoichiometric amounts of 1.02:1 in $LiOH$ and $Ni_{0.8}Co_{0.1}Mn_{0.1}(OH)_2$, followed by a heat-treatment procedure at 800°C for 20 h in a stream of dried air. An excess amount of Li was used to compensate for the loss of Li during firing. (The resultant powders showed a BET surface area of 1.0 m^2/g, while that of the powders prepared from the sol-gel method was 2.1 m^2/g.) In order to coat the $AlPO_4$ particles on the $LiNi_{0.8}Co_{0.1}Mn_{0.1}O_2$ cathode, 3 g of $Al(NO_3)_3 \cdot 9H_2O$ and 1 g of $(NH_4)_2HPO_4$ were slowly dissolved in 20 g of water until a white $AlPO_4$ nanoparticle suspension could be observed. The X-ray diffraction (XRD) patterns of the $AlPO_4$ nanoparticles annealed at 700°C showed orthorhombic crystalline phase (JCPDS 48-0652) with the chemical composition of $Al_1P_1O_4$. Fifty grams of $LiNi_{0.8}Co_{0.1}Mn_{0.1}O_2$ with an average particle size of ~13 μm were added to the coating solution and thoroughly mixed for 5 min. The slurry was then dried in an oven at 120°C for 6 h, and heat-treated in a furnace at 700°C for 5 h. Electron probe microanalysis (EPMA) mapping (with cross-sectioned powders) and Auger electron spectroscopy (with sputtering) confirmed the nanoscale coating layer, consistent with the previous results.[17,21] For the Al_2O_3 coating on a bare cathode, the same coating procedure was used with the previous work.[22] Five grams of Al-isopropoxide was first dissolved in isopropanol, and a bare cathode (100 g) was slowly added and mixed for 10 min. The mixture was dried and heat-treated at 130 and 700°C for 10 and 5 h, respectively.

The particle shapes and morphologies of the bare and $AlPO_4$-coated powders are shown in Fig. 1a and b, respectively. After coating the particles with $AlPO_4$, the surface morphology of the particle showed densely packed, rock-shaped grains. This indicates that the $AlPO_4$ nanoparticles had partially reacted with the $LiNi_{0.8}Co_{0.1}Mn_{0.1}O_2$ during firing at 700°C. Auger electron spectroscopy (AES) and transmission electron microscopy (TEM) demonstrated that the $AlPO_4$ coating thickness was approximately 10 nm.[17,23]

Preparation of test cells.—Cathodes for battery test cells were made from the active material (~25 mg), Super-P carbon black (MMM, Belgium), and a polyvinylidene fluoride (PVDF) binder (Kureha Company) at a weight ratio of 96:2:2. A cathode slurry was prepared by thoroughly mixing a *N*-methyl-2-pyrrolidene (NMP) solution with the PVDF, the carbon black, and the powdery cathode active material. The electrodes were prepared by coating the cathode-slurry onto an Al foil, followed by drying at 130°C for 20 min. Coin-type battery test cells (size 2016) containing a cathode, a

Li metal anode, and a microporous polyethylene separator were prepared in a helium-filled glove box. The electrolyte used was 1 M $LiPF_6$ with ethylene carbonate/diethylene carbonate/ethylmethyl carbonate (EC/DEC/EMC) (30:30:40 vol %). After the addition of the electrolyte, the test cells were aged at room temperature for 24 h before commencing the electrochemical tests.

Li-ion cells with a 840 mAh standard capacity [cell size: 3.4 × 40 × 62 mm^3 (thickness × length × width)] were used for the 4.35 V nail penetration and 12 V overcharging tests, and the test procedure followed the guidelines.[15] Bare and $AlPO_4$ nanoparticle-coated $LiNi_{0.8}Co_{0.1}Mn_{0.1}O_2$ were used as the cathode, and the anode material was synthetic graphite. The cell surface temperature was monitored using a K-type thermocouple placed on the center of the largest face in the cell can, and the thermocouple was tightly glued with an insulating tape.

Electrochemical and DSC tests.—In order to compare the capacity of the bare and $AlPO_4$-coated $LiNi_{0.8}Co_{0.1}Mn_{0.1}O_2$ cathodes, coin-type half cells were used with a charge cutoff voltage of 4.3 V at the charge and discharge rates of 0.1 C (=18 mA/g). The cycle-life performance of the Li-ion cells was tested at 1 C rate for 200 cycles at 21°C. The rate capability tests of the Li-ion cells were carried out by varying the discharge rate with 0.2, 0.5, 1, or 2 C (while the charge rate was fixed at 1 C).

Differential scanning calorimetry (DSC) samples of the cathodes were prepared by charging the coin cells to 4.5 V at a 0.1 C rate, followed by holding them at that potential for 5 h. These cells were then disassembled in a glove box to get the charged cathode part, which typically contained ~35 wt % electrolyte, ~25 wt % Al foil, ~2 wt % combined binder and carbon black, and ~38 wt % active material. The heating rate of the DSC experiment was 3°C/min.

Li-ion full cells for the DSC experiments of the cathodes were charged to the predetermined cell voltages of 4.2 and 4.6 V (corresponding to ~4.3 and ~4.7 V *vs.* Li metal, respectively) at a constant-current mode (1 C rate), followed by holding these voltages until the currents decreased to 30 mA ($\approx$1/30 C). The charged cathodes were then disassembled from the cells in a dry room. Approximately 10 mg of the cathode was hermetically sealed in an aluminum DSC sample pan, and the scan rate was 3°C/min. Only the cathode material was used to calculate specific heat flow.

X-ray diffraction (XRD).—A M18XHF-SRA diffractometer (MACScience Co.) with a Cu target tube was used for XRD measurement with a graphite monochromator. The scattered X-rays for the range of 15° < 2θ < 70° were detected for every 0.02° increment.

Results and Discussion

The XRD patterns of the bare and $AlPO_4$-coated $LiNi_{0.8}Co_{0.1}Mn_{0.1}O_2$ materials are shown in Fig. 2. Both materials are indexed to the hexagonal-type structural group ($R\bar{3}m$). The lattice constants a and c for the $AlPO_4$-coated $LiNi_{0.8}Co_{0.1}Mn_{0.1}O_2$ material are 2.8782 ± 0.0004 and 14.217 ± 0.004 Å, respectively, having similar values to the bare one, $a = 2.8766 \pm 0.0003$ Å and $c = 14.219 \pm 0.003$ Å.

Figure 3 shows the XRD patterns of the $AlPO_4$-coated $Li_xNi_{0.8}Co_{0.1}Mn_{0.1}O_2$ cathode electrodes at 4.2, 4.4, 4.6, and 4.8 V (during the first charge) in the Li-ion cells with a carbon anode (corresponding to approximately 0.1 V higher voltage *vs.* Li metal, respectively). The shift in the (003) peaks is noticeable in the XRD patterns of the charged $AlPO_4$-coated $Li_xNi_{0.8}Co_{0.1}Mn_{0.1}O_2$. The (003) peak shifts toward a lower angle during the charging up to 4.2 V, and then shifts back to a higher angle as Li ions are further deintercalated. In addition, the (009) and (107) peaks are observed to shift to higher angles. Ohzuku *et al.*[24] and Li *et al.*[25] reported that delithiated Li_xNiO_2 ($x \sim 0$) maintained its hexagonal structure. Similarly, the XRD patterns of the bare and $AlPO_4$-coated $Li_xNi_{0.8}Co_{0.1}Mn_{0.1}O_2$ remains as $R\bar{3}m$ at $x \sim 0$ (4.8 V), and the
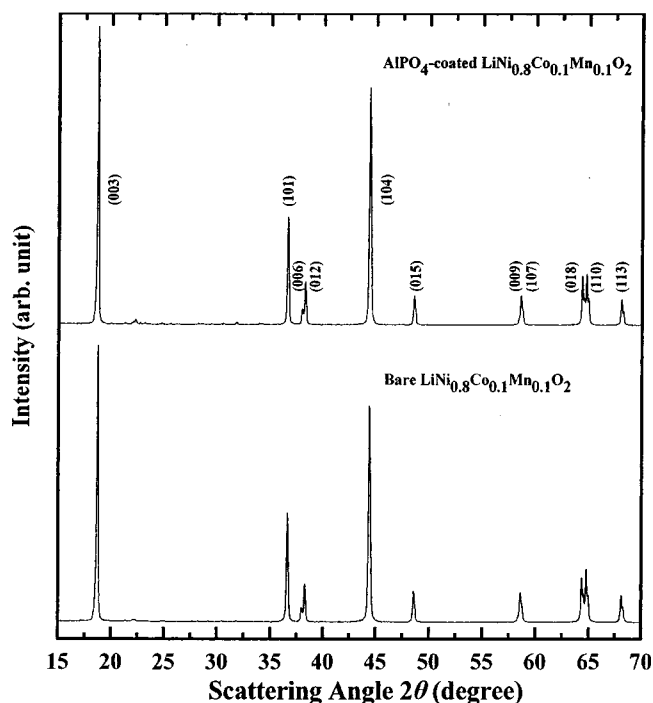
Figure 2. XRD patterns of the bare and AlPO$_4$-coated LiNi$_{0.8}$Co$_{0.1}$Mn$_{0.1}$O$_2$ powders.

conversion to the O 1 type structure at x $\sim$ 0 does not develop while the LiCoO$_2$ structure does. Evolution of the XRD patterns of the bare cathode was similar to those of the AlPO$_4$-coated cathode.

The discharge curves of the bare and AlPO$_4$-coated LiNi$_{0.8}$Co$_{0.1}$Mn$_{0.1}$O$_2$ between 4.3 and 3 V at a rate of 0.1 C (with coin-type test cells using Li-metal anode) are compared in Fig. 4a. Both samples exhibit a discharge capacity of 188 mAh/g. Figure 4b shows the DSC scans of the bare, AlPO$_4$-, and Al$_2$O$_3$-coated Li$_x$Ni$_{0.8}$Co$_{0.1}$Mn$_{0.1}$O$_2$ electrodes charged at 4.5 V (using a Li metal anode). The inset is the voltage curve during the charge to 4.5 V of

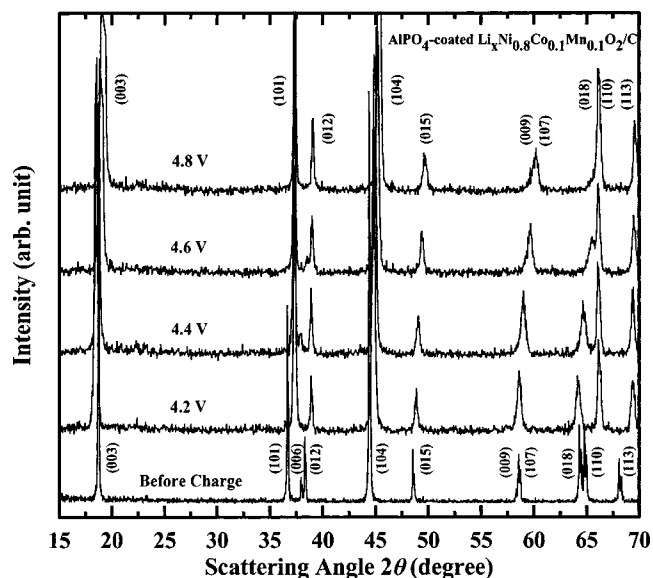**Figure 3.** XRD patterns of the AlPO$_4$-coated Li$_x$Ni$_{0.8}$Co$_{0.1}$Mn$_{0.1}$O$_2$ cathode material as a function of the charge voltage.
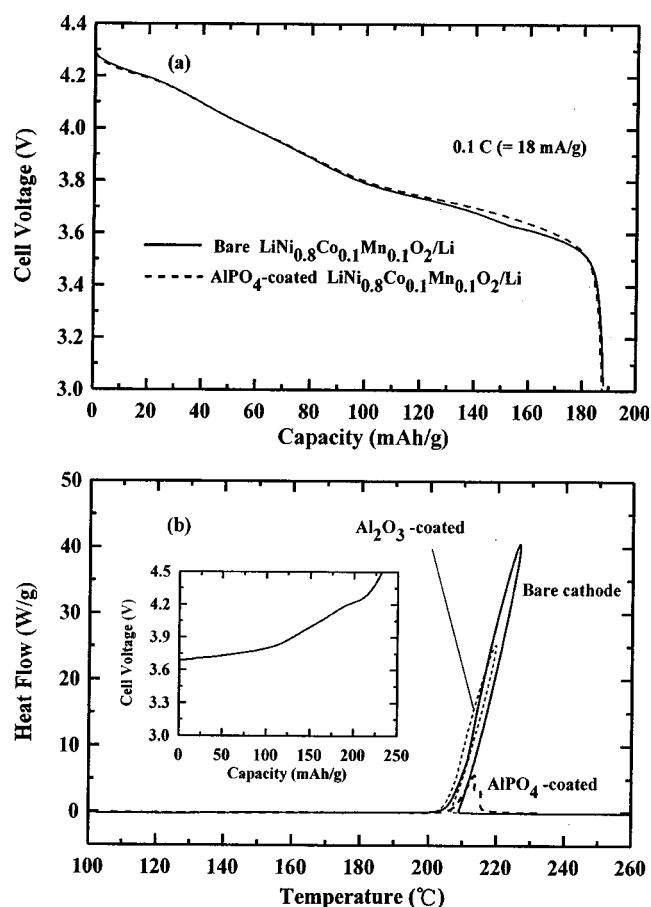

Figure 4. Plots of (a) discharge curves of the bare and AlPO$_4$-coated LiNi$_{0.8}$Co$_{0.1}$Mn$_{0.1}$O$_2$ cathodes in the coin-type half cells between 4.3 and 3 V at 0.1 C rate (=18 mA/g), and (b) DSC scans of the bare, AlPO$_4$-, and Al$_2$O$_3$-coated Li$_x$Ni$_{0.8}$Co$_{0.1}$Mn$_{0.1}$O$_2$ cathodes at 4.5 V (with a Li metal anode).

bare LiNi$_{0.8}$Co$_{0.1}$Mn$_{0.1}$O$_2$ cathode, showing the charge capacity of 235 mAh/g. The bare LiNi$_{0.8}$Co$_{0.1}$Mn$_{0.1}$O$_2$ cathode exhibits a steeply rising heat flow height up to 40 W/g beginning at ~200°C. This is a great concern during the thermal abuse tests in Li-ion cells, because rapid heat generation from the decomposition of the cathode in a very short time can be much faster than the heat dissipation to the environment, which causes thermal runaway.[26] However, the AlPO$_4$-coated LiNi$_{0.8}$Co$_{0.1}$Mn$_{0.1}$O$_2$ shows more diffused exothermic heat, with only a quarter of that observed in the bare cathode. In addition, the Al$_2$O$_3$-coated cathode produces approximately double the heat than that of AlPO$_4$-coated LiNi$_{0.8}$Co$_{0.1}$Mn$_{0.1}$O$_2$. These indicate that the degree of heat generation strongly depends on the coating materials; the AlPO$_4$ coating layer minimizes the exothermic reaction of the cathode with the electrolyte, which triggers the violent evolution of oxygen generation from the cathode.

These thermal results correlate with the nail penetration tests of Li-ion cells at 4.35 V charge (corresponding to ~4.5 V *vs.* Li metal), which is considered to stimulate an internal short in Li-ion cells. This test directly shows the thermal stability of the cathodes because a sudden internal short accompanying an abrupt increase in joule heat is induced. Figure 5 shows the cell appearance after the test. A maximum surface temperature of ~400°C was observed in the cell with the bare LiNi$_{0.8}$Co$_{0.1}$Mn$_{0.1}$O$_2$ with accompanying sparks and fire, while the cell with the AlPO$_4$-coated cathode showed a maximum temperature of ~80°C without thermal runaway.

In order to investigate the thermal properties of the cathodes at different overcharge states, the DSC scans of the bare and
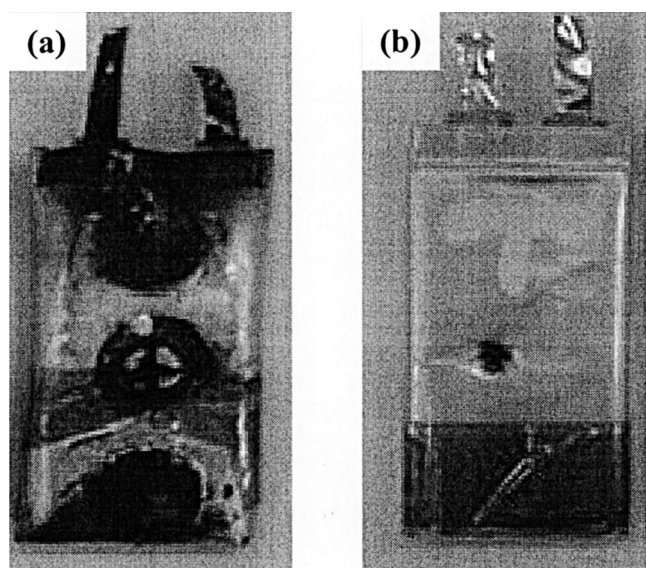
Figure 5. External appearance of the Li-ion cells of (a) bare and (b) AlPO$_4$-coated LiNi$_{0.8}$Co$_{0.1}$Mn$_{0.1}$O$_2$ cathodes after finishing the nail penetration test at 4.35 V charge.

AlPO$_4$-coated LiNi$_{0.8}$Co$_{0.1}$Mn$_{0.1}$O$_2$ cathodes are compared in Fig. 6, which were obtained from the Li-ion cells with a carbon anode at 4.2 and 4.6 V (corresponding to ~4.3 and ~4.7 V *vs.* Li metal, respectively). As the charge voltage increases, the major exothermic
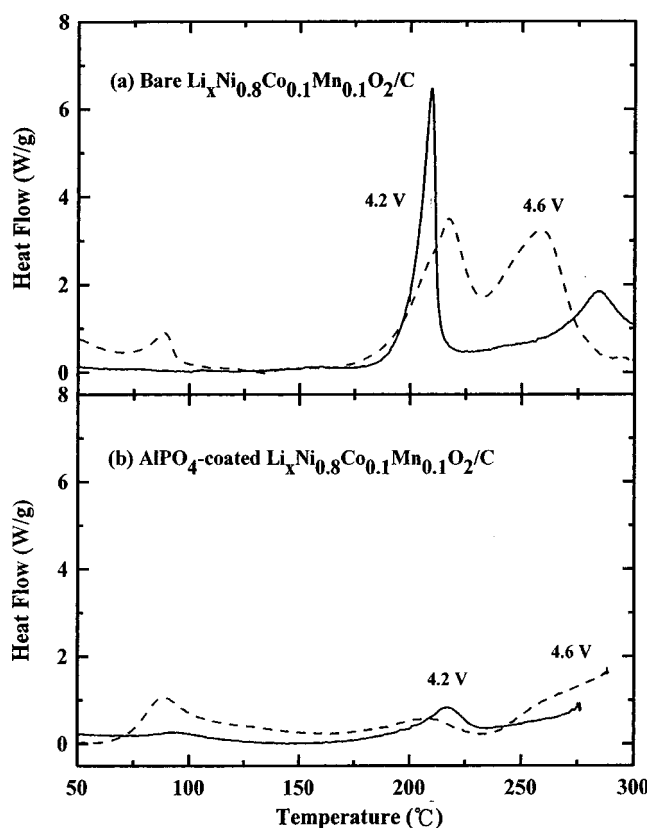

Figure 6. DSC scans of the bare and AlPO$_4$-coated LiNi$_{0.8}$Co$_{0.1}$Mn$_{0.1}$O$_2$ cathodes at 4.2 and 4.6 V *vs.* carbon (~4.3 and ~4.7 V *vs.* lithium, respectively). The cathodes were extracted from the Li-ion cells, and the scan rate was 3°C/min.
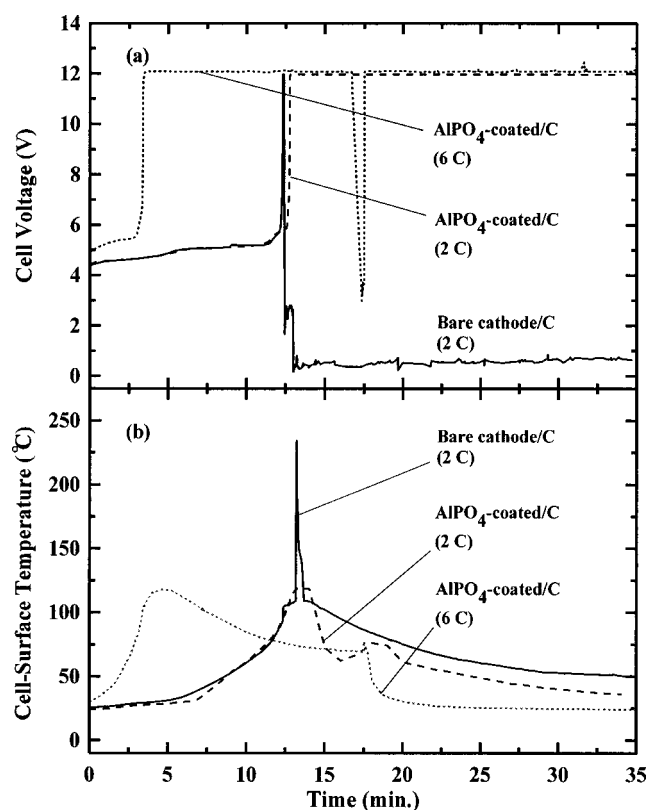

Figure 7. Plots of the cell voltage and cell surface temperature in the Li-ion cells containing bare and AlPO$_4$-coated LiNi$_{0.8}$Co$_{0.1}$Mn$_{0.1}$O$_2$ cathodes as a function of time at 2 C and 6 C rates during the 12 V overcharge test.

peaks at around 200°C in the bare Li$_x$Ni$_{0.8}$Co$_{0.1}$Mn$_{0.1}$O$_2$ are split, which is probably related to the slower reaction kinetics. However, the total heat generation increases with more delithiation in the bare Li$_x$Ni$_{0.8}$Co$_{0.1}$Mn$_{0.1}$O$_2$, showing similar trends of undoped Li$_x$NiO$_2$ cathode.[27,28] The AlPO$_4$ coating leads to significantly reduced exothermic heat, which is only *ca.* one-quarter of the bare cathodes at both charge voltages. It is believed that the covalent bonding nature of (PO$_4$)$^{3-}$ with the Al cation leads to strong resistance to the reaction with the electrolyte, and oxides with (PO$_4$)$^{3-}$ bonding have been reported to be thermally stable.[29,30] Moreover, the decrease of cathode surface exposed to the electrolyte plays a role in reducing the oxygen generation. More detailed studies on the nature of the coating layer for thermal passivation against the exothermic reaction with the electrolyte are currently underway.

While the nail penetration test is sensitive to the thermal stability of the cathode at very short times, the 12 V overcharge tests are sensitive to the cumulative heat generation of the cathode during a longer time, because a continuous current is applied even after all the lithium ions have been removed from the cathode. In order to evaluate the effect of heat generation from the bare and AlPO$_4$-coated LiNi$_{0.8}$Co$_{0.1}$Mn$_{0.1}$O$_2$ on the Li-ion cells during the 12 V overcharge, the cells containing cathodes were charged to 12 V at the 2 and 6 C rates (Fig. 7). At a higher C rate, the cell temperature increases rapidly due to accelerated electrolyte oxidation, cathode decomposition, and other cell component reactions by the rapid increase of joule heat. Among these, the cathode decomposition reaction was reported to trigger a thermal runaway of the cell.[31,32] A Li-ion cell containing bare LiNi$_{0.8}$Co$_{0.1}$Mn$_{0.1}$O$_2$ cathode exhibits a cell surface temperature of up to approximately 250°C, accompanying by smoke with the bottom of the can ruptured. On the other hand, the AlPO$_4$-coated LiNi$_{0.8}$Co$_{0.1}$Mn$_{0.1}$O$_2$ cathode is limited to a maximum temperature of ~110°C. Even at the extreme case of a high current corresponding to 6 C (≈5 A) applied to the cell con-
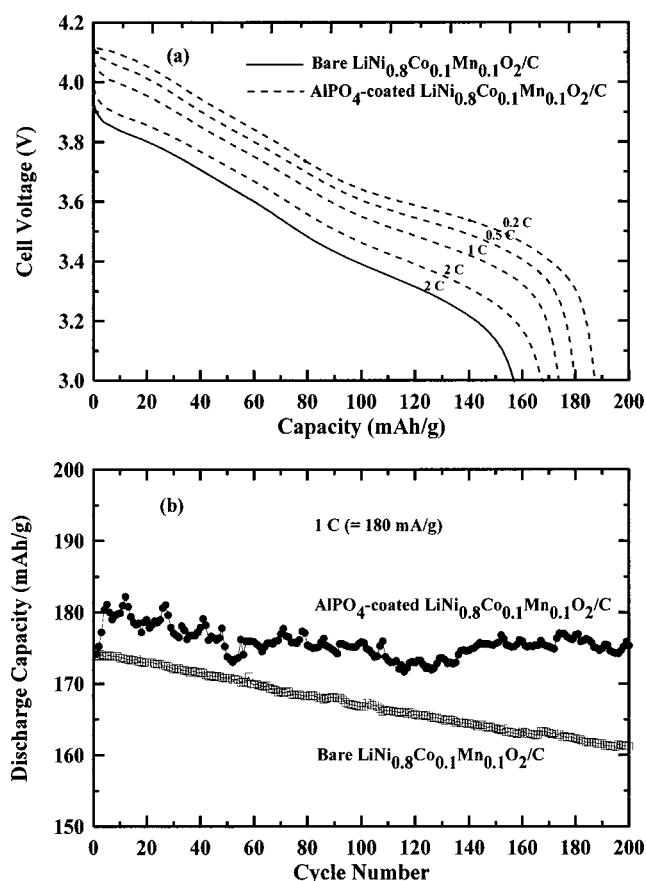
Figure 8. Plots of (a) discharge curves of the bare and $AlPO_4$-coated $LiNi_{0.8}Co_{0.1}Mn_{0.1}O_2$ cathodes in Li-ion cells at various C rates between 4.2 and 3 V, and (b) discharge capacities of the bare and coated cathodes as a function of cycle number.

taining $AlPO_4$-coated $LiNi_{0.8}Co_{0.1}Mn_{0.1}O_2$ cathode, the cell does not show thermal runaway, and the cell surface temperature is similar to the 2 C rate case. In this condition, all the exothermic decomposition reactions of the cell components occur within $\sim$5 min, but the cell remains stable suggesting that the amount of heat generated from the cathode is an indication of whether or not a catastrophic failure of the cell will occur. Note that the cell does not show an abrupt temperature increase although there is a sudden short-circuit at $\sim$17 min. For the 12 V overcharge experiments, five cells were tested for each condition, and the results were reproducible.

Figure 8a shows the discharge curves of the bare and $AlPO_4$-coated $LiNi_{0.8}Co_{0.1}Mn_{0.1}O_2$ by increasing the discharge rate from 0.2 to 0.5, 1, and 2 C rates. The discharge curve of the coated cathode is better than the uncoated one, and similar behavior was observed in the Al_2O_3-coated $LiCoO_2$.[22] The capacity retention of the Li-ion cell between 4.2 and 3 V is $\sim$100% with the $AlPO_4$-coated $LiNi_{0.8}Co_{0.1}Mn_{0.1}O_2$, while that of the bare cathode is 92% after 200 cycles, as shown in Fig. 8b. In the bare $LiNi_{0.8}Co_{0.1}Mn_{0.1}O_2$, the concentrations of dissolved Co and Ni were 80 and 20 ppm after cycling, respectively, with negligible Mn dissolution. Amatucci *et al.* reported that cobalt dissolution is closely related to the weakening of the crystal structure by the removal of the binding lithium.[33] However, the $AlPO_4$ coating layer blocks the potential HF attack from the electrolyte.[34] Improved rate capability and cycle life performance may be also partially associated with the catalytic effect of $AlPO_4$-coating layer to dissolve Li ions in the electrolyte.

We consider a pH change of cathode powders immersed in NMP (normally containing $\sim$0.5 wt % water). In contrast to $LiCoO_2$, Li
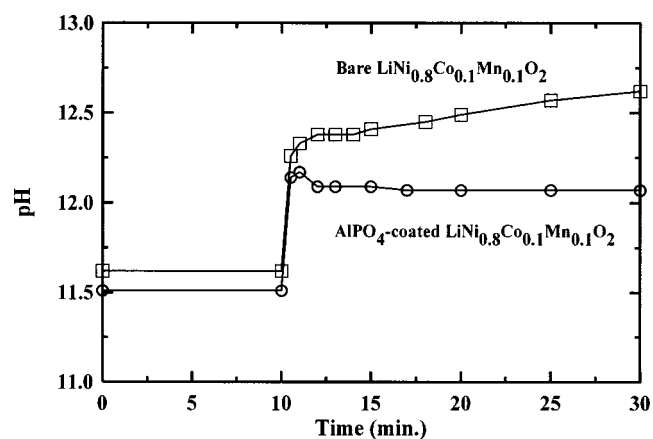

Figure 9. Plots of the pH changes in the NMP solution (with 0.5 wt % water content) containing the bare or $AlPO_4$-coated $LiNi_{0.8}Co_{0.1}Mn_{0.1}O_2$ materials.

ions in Ni-based cathodes were easily extracted through contact with water. This was critical for preparing the cathode slurry since the dissolution of Li from the cathode induced an increase in the pH of the slurry, thus increasing the viscosity of slurry over 10,000 poise within 30 min. (Normally the slurry viscosity should be stabilized within $\sim$5000 poise.) As shown in Fig. 9, the pH of both NMP solutions abruptly increased from 11.5 to 12 at 10 min after immersing each cathode into the NMP solution. However, after that, the pH of solution in the bare $LiNi_{0.8}Co_{0.1}Mn_{0.1}O_2$ continued to increase, which is in contrast to the coated cathode case. This suggests that the $AlPO_4$-nanoscale coating layer blocks lithium dissolution from the powder surface.

Conclusions

An $AlPO_4$-nanoscale coating on the $LiNi_{0.8}Co_{0.1}Mn_{0.1}O_2$ cathode improved both the thermal stability and electrochemical properties. Coated $LiNi_{0.8}Co_{0.1}Mn_{0.1}O_2$ material had a noticeably reduced exothermic reaction of the cathode with the electrolyte, without sacrificing the specific capacity of the bare $LiNi_{0.8}Co_{0.1}Mn_{0.1}O_2$. These results are consistent with the thermal abuse tests of Li-ion cells.

Acknowledgment

References

1. W. Li, J. N. Reimers, and J. R. Dahn, *Solid State Ionics,* **67**, 123 (1993).
2. J. Cho, G. Kim, Y. Park, and S. Kim, U.S. Pat. 62,419,59 (2001).
3. Y. Nishida, K. Nakane, and T. Satoh, *J. Power Sources,* **68**, 561 (1997).
4. H. Watanabe, T. Sunagawa, H. Fujimoto, N. Nishida, and T. Nohma, *Sanyo Tech. Rev.,* **30**, 84 (1998).
5. Y. Sato, T. Koyano, M. Mukai, and K. Kobayakawa, Abstract 109, The Electrochemical Society Meeting Abstracts, Vol. 97-2, Paris, France, Aug 31-Sept 5, 1997.
6. M. Yoshio, H. Noguchi, J.-I. Itoh, M. Okada, and T. Mouri, *J. Power Sources,* **90**, 176 (2000).
7. C. Nayoze, F. Ansart, C. Laberty, J. Sarrias, and A. Rousset, *J. Power Sources,* **99**, 54 (2001).
8. J. Cho, H. Jung, Y. Park, G. Kim, and H. S. Lim, *J. Electrochem. Soc.,* **147**, 15 (2000).
9. J. Cho, G. Kim, and H. S. Lim, *J. Electrochem. Soc.,* **146**, 3571 (1999).
10. W. Li and J. C. Currie, *J. Electrochem. Soc.,* **144**, 2773 (1997).
11. C. Delmas, I. Saadoune, and A. Rougier, *J. Power Sources,* **44**, 595 (1993).
12. A. Ueda and T. Ohzuku, *J. Electrochem. Soc.,* **141**, 2010 (1994).
13. Y. Gao, M. V. Yakovleva, and W. B. Ebner, *Electrochem. Solid-State Lett.,* **1**, 117 (1998).
14. U. Isozaki, K. Kubo, S. Yamada, and M. Kanda, Abstract 143, The Electrochemical Society Meeting Abstracts, Vol. 2002-2, Salt Lake City, Utah, Oct 20-24, 2002.
15. *Guideline for the Safety Evaluation of Secondary Lithium Cells*, Japan Battery Association (1997).

16. N. Takami, H. Inagaki, H. Ishii, R. Ueno, and M. Kanda, Abstract 371 of 11th International Meeting on Lithium Batteries (2002).
17. J. Cho, Y.-W. Kim, B. Kim, J.-G. Lee, and B. Park, *Angew. Chem., Int. Ed. Engl.,* **42**, 1618 (2003).
18. J. Cho, Y. Park, and G. Kim, U.S. Pat. pending.
19. N. Yabuuchi and T. Ohzuku, *J. Power Sources,* **119-121**, 171 (2003).
20. Z. Lu, D. D. MacNeil, and J. R. Dahn, *Electrochem. Solid-State Lett.,* **4**, A200 (2001).
21. T.-J. Kim, D. Son, J. Cho, B. Park, and H. Yang, *Electrochim. Acta,* **49**. 4405 (2004).
22. J. Cho, Y. J. Kim, and B. Park, *Chem. Mater.,* **12**, 3788 (2000).
23. J. Cho, T.-J. Kim, T.-G. Kim, C. Kim, and B. Park, Unpublished results.
24. T. Ohzuku, A. Ueda, and M. Nagayama, *J. Electrochem. Soc.,* **140**, 1862 (1993).
25. W. Li, J. N. Reimers, and J. R. Dahn, *Solid State Ionics,* **67**, 123 (1993).
26. S. C. Levy and P. Bro, *Battery Hazards and Accident Prevention*, Plenum Press, New York (1994).

27. J. R. Dahn, E. W. Fuller, M. Obrovac, and U. von Sacken, *Solid State Ionics,* **69**, 265 (1994).
28. Z. Zhang, D. Fouchard, and J. R. Rea, *J. Power Sources,* **70**, 16 (1998).
29. A. K. Padhi, K. S. Nanjundaswamy, and J. B. Goodenough, *J. Electrochem. Soc.,* **144**, 1188 (1997).
30. S. Okada, S. Sawa, M. Egashira, J.-I. Yamaki, M. Tabuchi, H. Kageyama, T. Konishi, and A. Yoshino, *J. Power Sources,* **97**, 430 (2001).
31. R. A. Leising, M. J. Palazzo, E. S. Takeuchi, and K. J. Takeuchi, *J. Electrochem. Soc.,* **148**, A838 (2001).
32. H. Maleki, S. A. Hallaj, J. R. Selman, R. B. Dinwiddie, and H. Wang, *J. Electrochem. Soc.,* **146**, 947 (1999).
33. G. G. Amatucci, J. M. Tarascon, and L. C. Klein, *Solid State Ionics,* **83**, 167 (1996).
34. A. M. Andersson, D. P. Abraham, R. Haasch, S. MacLaren, J. Liu, and K. Amine, *J. Electrochem. Soc.,* **149**, A1358 (2002).